Copyright © 2009. Reprinted from APPLIED PHYSICS LETTERS.91,051905.2007. Such permission of the American Institute of Physics does not in any way imply the American Institute of Physics endorsement of any of Institute of Microelectronics' products or services. Internal or personal use of this material is permitted. However, permission to reprint/republish this material for advertising or promotional purposes or for creating new collective works for resale or redistribution must be obtained from the American Institute of Physics by writing to Rights@aip.org.

Enhanced thermal stability of nickel germanide on thin epitaxial germanium by adding an ultrathin titanium layer

Shiyang Zhu,[a] M. B. Yu, G. Q. Lo, and D. L. Kwong
Institute of Microelectronics, 11 Science Park Road, Singapore 117685, Singapore

(Received 29 May 2007; accepted 12 July 2007; published online 31 July 2007)

The thermal stability of NiGe films formed on epitaxial Ge on Si substrates was improved from 450 to 550 °C by simply adding an ultrathin (~1 nm) Ti layer during Ni deposition, either as an intermediate layer between Ni and Ge or as a capping layer on Ni. The improvement was attributed to the formation of ternary $Ni_{1-x}Ti_xGe$ phase near the NiGe surface, which acts as a capping layer to suppress agglomeration of the underlying NiGe film at an elevated temperature, as well as modification of the NiGe grain boundaries. The resistivity of NiGe is also slightly reduced by the Ti incorporation, making this method very promising for the germanium technology. © *2007 American Institute of Physics*. [DOI: 10.1063/1.2768203]

Germanium is an attractive material both for being metal-oxide-semiconductor transistor channel material for its high carrier mobility[1] and being infrared photodetector's absorbing layer at $\lambda = 1.3-1.55$ μm due to its small direct energy band gap of 0.8 eV.[2] As in the conventional Si technology where self-aligned metal silicide is used for the source/drain contact and local interconnect, self-aligned metal germanide should be also necessary for the Ge devices fabrication. NiGe is one of the most promising candidates due to its low resistivity, low formation temperature, and feasibility for self-aligned fabrication.[3–5] However, one major drawback of NiGe is its low thermal stability due to agglomeration, about 500–550 °C for NiGe on bulk Ge and even lower for that on polycrystalline or amorphous Ge.[6–8] It was reported that the thermal stability of NiGe on bulk Ge may be improved by Zr alloying to Ni.[9] However, Zr is not a commonly used metal in the conventional self-aligned silicide process. On the other hand, in a viewpoint of compatibility to the well developed Si technology as well as being cost effective, epitaxial Ge on Si is more promising than the bulk Ge. High quality heteroepitaxial Ge film has been grown on Si recently using molecular beam epitaxy[2] or ultrahigh vacuum chemical vapor deposition[10] (UHVCVD) in spite of ~4% lattice mismatch between Ge and Si. In this letter, we demonstrated that the thermal stability of NiGe on epitaxial Ge can be significantly enhanced by simply adding an ultrathin Ti(~1 nm) layer during Ni deposition, either as an intermediate layer or as a capping layer.

The strain-relaxed Ge epilayer was grown on Si substrate using a recently developed two-step UHVCVD epitaxial technology.[11] First, ~30 nm Ge buffer layer was deposited at 250–350 °C using diluted GeH_4 source, and then ~100 nm Ge epilayer was grown at 600–700 °C. No cycling annealing was carried out after the growth. The as-formed Ge epilayer has been confirmed to have high quality with the dislocation density of $<10^7$ cm^{-2} and the surface rms roughness of ~1.0 nm in a 10×10 μm^2 scanning area.[11] After dipping the wafers in a diluted HF solution to remove the native oxide, they were immediately loaded in a sputtering system where Ni and Ti were deposited sequentially without breaking the vacuum. Three sets of samples were deposited: pure Ni(~9 nm), Ni(~9 nm)/Ti(~1 nm) (Ti as an intermediate layer between Ni and Ge), and Ti (~1 nm)/Ni(~9 nm) (Ti as a capping layer on Ni). Ni–Ge reaction on the blank and patterned wafers was performed through *ex situ* rapid thermal annealing (RTA) at 350 °C for 30 s in N_2 ambient, followed by selectively etching (SE) in a diluted HNO_3 solution to remove unreacted metal. Then, the wafers were split to small pieces and each piece was performed by second RTA in vacuum for 30 s at various temperatures ranging from 350 to 700 °C. In other experiment, the wafers were accumulatively annealed in N_2 ambient for 30 s at temperatures of 350, 400, 500, and 600 °C.

After the first 350 °C RTA and SE, all samples showed smooth surface. The rms roughness is about 0.7–0.9 nm as measured from atomic force microscopy (AFM) for a scanning area of 5×5 μm^2, similar to the initial Ge epilayer. The roughness after the second vacuum RTA is shown in Fig. 1 as a function of temperature. For the pure Ni samples, the roughness starts to increase at 450 °C, reaches to 1.7 nm at 500 °C, and abruptly reaches to 8.9 nm at 550 °C, whereas the Ti incorporated samples moderately increase their roughness from 1.2 nm at 500 °C to 3.5 nm at 650 °C. The samples after the accumulative RTA process exhibit similar

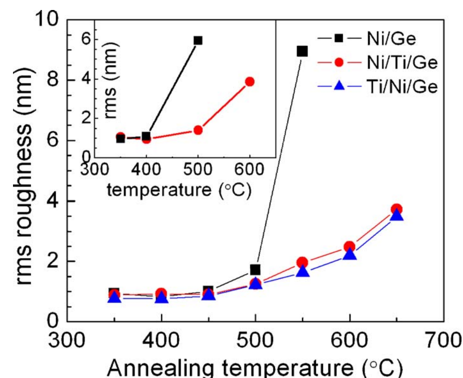

FIG. 1. (Color online) rms roughness determined from AFM in a scanning area of 5×5 μm^2 as a function of second vacuum RTA temperature for NiGe films formed from Ni(9 nm), Ni(9 nm)/Ti(1 nm), and Ti(1 nm)/Ni(9 nm). The inset shows rms of Ni(9 nm) and Ni(9 nm)/Ti(1 nm) samples after accumulative RTA in N_2 ambient, its slightly faster increase rate with temperature may arise from its longer accumulated annealing time.

[a]Electronic mail: zhusy@ime.a-star.edu.sg

0003-6951/2007/91(5)/051905/3/$23.00

© 2007 American Institute of Physics
Downloaded 31 Jul 2007 to 202.6.242.69. Redistribution subject to AIP license or copyright, see http://apl.aip.org/apl/copyright.jsp

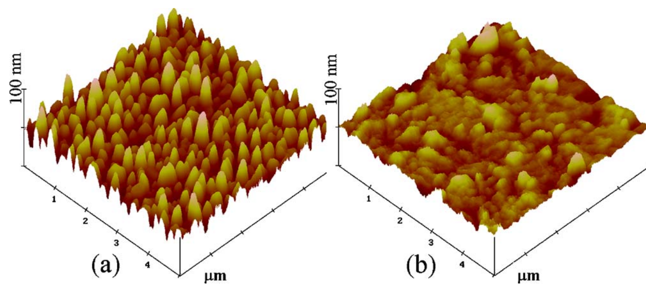

FIG. 2. (Color online) AFM surface morphologies with the scanning area of $5\times5\ \mu m^2$ of (a) 550 °C annealed Ni(9 nm) sample, it contains regularly distributed isolated islands with a rms of 8.9 nm, and (b) 650 °C annealed Ni(9 nm)/Ti(1 nm) sample, it contains some irregularly distributed hills and grooves with a rms of 3.7 nm.

trend, as shown in the inset of Fig. 1. Moreover, different sets of samples exhibit different roughened surface morphologies, as observed from the AFM images in Fig. 2 for the 550 °C annealed pure Ni sample and 650 °C annealed Ti intermediated sample. Figure 3 compares scanning electron microscopy (SEM) images of the three sets of samples just before and after the surface being significantly roughened, i.e., pure Ni samples annealed at 450 and 500 °C and Ni/Ti and Ti/Ni samples annealed at 500 and 600 °C. The pure Ni samples show NiGe grain coarsening at 450 °C, and clearly agglomerates into isolated islands with the size of ~130 nm at 500 °C. The NiGe island formation was confirmed by the energy dispersive x-ray (EDX) fluorescence spectroscopy measurement, as both Ni and Ge signals were detected within the island area whereas no Ni (only Ge) signal was detected outside the island area. For the Ti intermediated samples, the surface is also textured, but no island formation even at 600 °C, as being consistent with the AFM observation. For the Ti capped samples, grain growth and agglomeration also occur at 600 °C, but not as significant as the 500 °C annealed pure Ni sample. Both Ni and Ge signals can be detected by EDX at any location of the 600 °C annealed Ni/Ti and Ti/Ni samples, indicating that the NiGe films are still continuous.

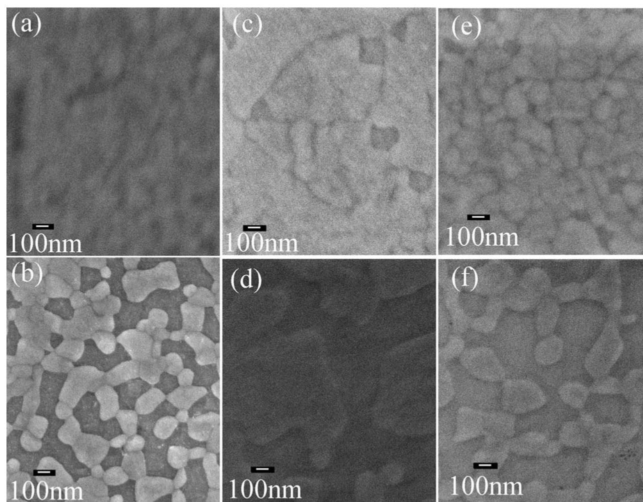

FIG. 3. SEM images of NiGe films formed from (a) Ni(9 nm) after 450 °C annealing, (b) Ni(9 nm) after 500 °C annealing, (c) Ni(9 nm)/Ti(1 nm) after 500 °C annealing, (d) Ni(9 nm)/Ti(1 nm) after 600 °C annealing, (e) Ti(1 nm)/Ni(9 nm) after 500 °C annealing, and (f) Ti(1 nm)/Ni(9 nm) after 600 °C annealing.

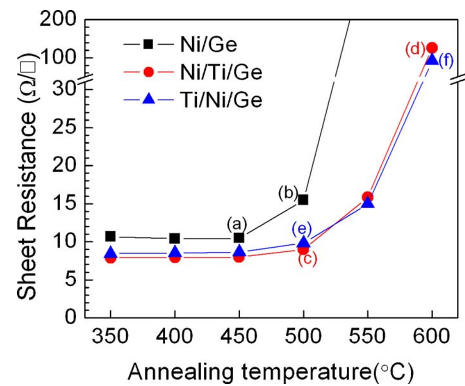

FIG. 4. (Color online) Sheet resistance as a function of second RTA temperature for NiGe films formed from Ni(9 nm), Ni(9 nm)/Ti(1 nm), and Ti(1 nm)/Ni(9 nm). The alphabetized points correspond to the SEM images shown in Fig. 3.

The sheet resistances ($R_{sq.}$) of NiGe are plotted in Fig. 4 as a function of annealing temperature for the aforementioned three sets of samples. $R_{sq.}$ is stable up to 450 °C for the pure Ni samples, and the stable range extends to 500 °C with the ultrathin Ti incorporation. The abrupt $R_{sq.}$ increase of the pure Ni samples can be attributed to the formation of isolated islands. However, the $R_{sq.}$ increase of the Ti incorporated samples may arise from other mechanism besides the NiGe agglomeration because the NiGe film is still continuous after 600 °C annealing. A possible mechanism is Ge outdiffusion to the NiGe surface and then oxidization.[12] This conjecture is partly confirmed by the fact that no Ni signal can be detected by EDX on the surface of 700 °C annealed NiGe samples with and without the Ti incorporation. Taking both resistivity and surface roughness into account, the thermal stability of NiGe can be extended to 550 °C by the ultrathin Ti incorporation, about 100 °C higher than that formed from pure Ni.

The formed NiGe films have thickness of approximate 23 nm, as observed from cross-sectional transmission electron microscopy (XTEM) on three 450 °C annealed samples. The resistivity is then calculated to be 24, 18, and 19 $\mu\Omega$ cm for NiGe formed from pure Ni, Ni/Ti, and Ti/Ni, respectively, close to the reported value (16–24 $\mu\Omega$ cm).[5,6] The slightly different resistivities among these three samples may be ascribed to their different NiGe grain sizes. From XTEM images, clear grain boundary can be observed, for instance, see Fig. 5(a). The distance between two grain boundaries can be roughly estimated to be ~180 nm for the pure Ni sample

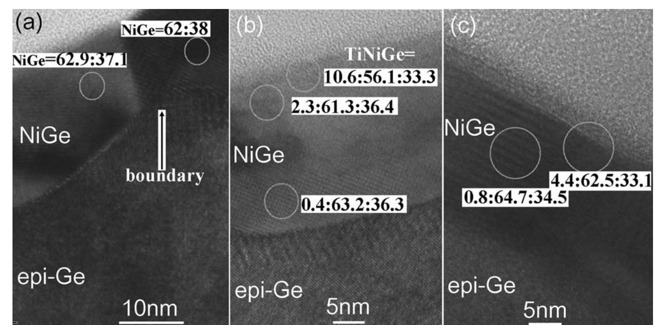

FIG. 5. High-resolution XTEM images of 450 °C annealed NiGe films formed from (a) Ni(9 nm), (b) Ni(9 nm)/Ti(1 nm), and (c) Ti(1 nm)/Ni(9 nm). The component ratio determined from EDX at various locations is also shown.

Downloaded 31 Jul 2007 to 202.6.242.69. Redistribution subject to AIP license or copyright, see http://apl.aip.org/apl/copyright.jsp

and ~320 nm for the Ti incorporated samples. Since the grain boundary can affect carrier transport, less grain density (due to larger grain size) results in a smaller resistivity. This is another benefit for the ultrathin Ti incorporation.

Figure 5 shows high-resolution XTEM images and elemental ratio at various locations determined from EDX for three 450 °C annealed samples. The ratio of Ni and Ge is about 1.6–1.8 for all three samples and at all locations, indicating that the formed germanide phase is Ni_5Ge_3. This phase was also observed for NiGe formed on amorphous and polycrystalline Ge.[4,5,13] For the Ti incorporated samples, Ti signal was detected, with higher concentration at closer surface region. Moreover, the Ti intermediated sample has higher Ti concentration than the Ti capped sample. This can be understood from the kinetics of Ni–Ge reaction. During the reaction of Ni–Ge system, Ni diffuses through the formed NiGe layer and reacts with Ge at the NiGe/Ge interface. The intermediate Ti layer is expelled to the surface and may alloy into the NiGe to form ternary $Ni_{1-x}Ti_xGe$ phase. For the Ti capped sample, part of Ti may remain unreacted during the first RTA and be removed by the subsequent SE, thus the Ti amount is reduced. Moreover, the Ti layer may reduce the NiGe growth rate by suppressing the supply rate of Ni to the NiGe/Ge interface, which may let the NiGe grain to grow to a large size, as in the case of Ni–Ti–Si system where epitaxial NiSi can be formed by an ultrathin Ti intermediate layer.[14]

The mechanism of Ti induced NiGe thermal stability enhancement may firstly be attributed to the ternary $Ni_{1-x}Ti_xGe$ at the surface, which acts as a capping layer to constrain the agglomeration of underlying NiGe film during the second RTA. Secondly, Ti alloying can decrease the Gibbs energy of the NiGe grain and/or change its grain boundary structure, thus improve the thermal stability, as in a Ni–Si system where it was reported that a small amount of Pt incorporation can improve the NiSi stability due to the reduction of the Gibbs energy.[15] Thirdly, less grain boundary density of the Ti incorporated NiGe films may also contribute their higher thermal stability because the driving force for NiGe agglomeration is the reduction of interfacial energy at the grain boundaries.[16] For NiGe formed on bulk Ge, we suspect that the same Ti induced thermal stability enhancement should also exist because the mechanisms for the enhancement still take effect.

From the AFM and SEM observations, we can find that Ti as an intermediate layer can suppress the NiGe agglomeration more effectively than Ti as a capping layer, but they exhibit similar thermal stability (roughness and resistivity). This may arise from the Ge epilayer related degradation due to agglomeration of the underlying Ge epilayer and/or outdiffusion of Ge atoms, which takes effect at about 550 °C for our samples.

Furthermore, it was reported that thinner NiGe on bulk Ge has lower thermal stability.[7] Similar trend is also found for our pure Ni samples on epitaxial Ge, as the pure Ni(5 nm) sample after 500 °C RTA has agglomerated to isolated islands with a rms of 5.95 nm, similar to the 550 °C annealed pure Ni(9 nm) sample. On the other hand, the Ni(3 nm)/Ti(1 nm) sample after 500 °C RTA has a rms of 0.85 nm, as smooth as the initial Ge film. Its thermal stability seems even slightly better than the Ni(9 nm)/Ti(1 nm) sample, probably due to its relatively large Ti ratio near the NiGe surface.

In conclusion, simply adding an ultrathin Ti layer during Ni deposition on epitaxial Ge on Si can significantly improve thermal stability and also slightly reduce resistivity of the formed NiGe film. The improvement is attributed to ternary $Ni_{1-x}Ti_xGe$ phase formed at the NiGe surface as well as modification of the grain boundary in the NiGe film. The effect becomes more significant for thinner NiGe films, making this method very promising in the germanium technology.

[1] S. Y. Zhu, R. Li, S. J. Lee, M. F. Li, A. Y. Du, J. Singh, C. X. Zhu, A. Chin, and D. L. Kwong, IEEE Electron Device Lett. **26**, 81 (2005).
[2] M. Jutzi, M. Berroth, G. Wohl, M. Oehme, and E. Kasper, IEEE Photonics Technol. Lett. **17**, 1510 (2005).
[3] S. Gaudet, C. Detavernier, C. Lavoie, and P. Desjardins, J. Appl. Phys. **100**, 034306 (2006).
[4] S. Gaudet, C. Detavernier, A. J. Kellock, P. Desjardins, and C. Lavoie, J. Vac. Sci. Technol. A **24**, 474 (2005).
[5] J. Y. Spann, R. A. Anderson, T. J. Thornton, G. Harris, S. G. Thomas, and C. Tracy, IEEE Electron Device Lett. **26**, 151 (2005).
[6] S. Y. Zhu and A. Nakajima, Jpn. J. Appl. Phys., Part 2 **44**, L753 (2005).
[7] Q. C. Zhang, N. Wu, T. Osipowicz, L. K. Bera, and C. Zhu, Jpn. J. Appl. Phys., Part 2 **44**, L1389 (2005).
[8] S. L. Hsu, C. H. Chien, M. J. Yang, R. H. Huang, C. C. Leu, and S. W. Shen, Appl. Phys. Lett. **86**, 251906 (2005).
[9] S. L. Liew, R. T. P. Lee, K. Y. Lee, B. Balakrisnan, S. Y. Chow, M. Y. Lai, and D. Z. Chi, Thin Solid Films **504**, 104 (2006).
[10] S. B. Samavedam, M. T. Currie, T. A. Langdo, and E. A. Fitzgerald, Appl. Phys. Lett. **73**, 2125 (1998).
[11] T. H. Loh, H. S. Nguyen, C. H. Tung, A. D. Trigg, G. Q. Lo, N. Balasubramanian, and D. L. Kwong, Appl. Phys. Lett. **90**, 092108 (2007).
[12] M. A. Rahman, T. Osipowicz, K. L. Pey, L. J. Jin, W. K. Choi, D. Z. Chi, D. A. Antoniadis, E. A. Fitzgerald, and D. M. Isaacson, Appl. Phys. Lett. **87**, 182116 (2005).
[13] F. Nemouchi, D. Mangelinck, J. L. Labar, M. Putero, C. Bergman, and P. Gas, Microelectron. Eng. **83**, 2101 (2006).
[14] O. Nakatsuka, K. Okubo, Y. Tsuchiya, A. Sakai, S. Zaima, and Y. Yasuda, Jpn. J. Appl. Phys., Part 1 **44**, 2945 (2005).
[15] D. Mangelinck, J. Y. Dai, J. S. Pan, and S. K. Lahiri, Appl. Phys. Lett. **75**, 1736 (1999).
[16] S. Nygren and S. Johansson, J. Appl. Phys. **68**, 1050 (1990).

Downloaded 31 Jul 2007 to 202.6.242.69. Redistribution subject to AIP license or copyright, see http://apl.aip.org/apl/copyright.jsp